Dean&Francis
ISSN 2959-6157

Cosmic ray muon tomography

Chongen Huang[1*],
Yaran Yang[2],
Zile Liu[3],
Zaiye Wang[4]
and Xiju Li[5]

[1] Basis International School PLH, Huizhou, 516200, China, Chongen.huang14030-basischinaa.com
[2] The Department of Mathematics, University of California, San Diego, 92092, U.S, yay025@ucsd.edu
[3] United World College of Changshu, Changshu, 215500, China, zlliu22@uwcchina.org
[4] Shijiazhuang No. 18 Middle School, Shijiazhuang, 050000, China, wangzaiye0406@outlook.com
[5] Chengdu Shude School, Chengdu, 610014, China, 1958885357@qq.com
*corresponding author

Abstract:
This study explores the application of cosmic ray muon tomography. It analyzes how cosmic ray detection can be used to obtain the shape and structure of absorber obstacle. We designed an experiment to obtain cosmic ray muon data with and without absorber. Through data analysis and comparison with python program, it can then be determined whether the result of analysis align with the hypothesis with physics principles and provide insightful evidence on the shape of the absorber.

Keywords: Cosmic ray, Muon tomography, Data Analysis.

1. Introduction

Muon tomography is a visual technology that use cosmic ray to detect the shape and structure of large object.

1.1 Summary of the use of muon tomography

We need to use specialized detectors which are capable of tracking the paths of muons as they pass through or are absorbed by the object. As muons travel through matter, they lose energy through interactions with the atomic nuclei and electrons in the material. Dense materials (like lead or uranium) will cause more absorption and scattering of muons compared to less dense materials. Then, we need to compare the incoming and outgoing trajectories of each muon which are recorded by the detectors. Using algorithms, the recorded data is processed to reconstruct a 3D image of the interior of the object.

ISSN 2959-6157

1.2 Applications of muon topography:

Pyramids: Muon tomography has been used to explore the interiors of pyramids to discover hidden chambers. For instance, it was used to identify a previously unknown void in the Great Pyramid of Giza.

Volcano Monitoring: By imaging the internal structure of volcanoes, scientists can study magma chambers and other internal features, which can help predict eruptions and understand volcanic processes.

2. 16 pairs cosmic watch analysis

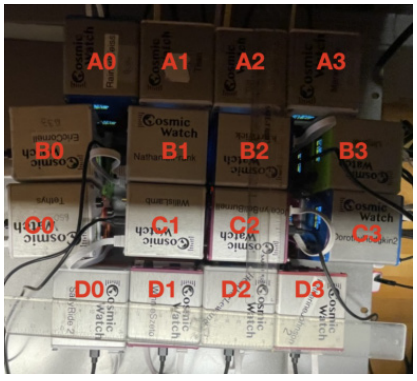

Figure 1 The arrangement of the detector

Our project aims to calculate, through coding and data analysis, and identify the shape and structure of the lead object(absorber). There are two sets of data collected in those 16 pairs of CW, two sets of data were collected. One set is empty detection with no object, and the other contains detection affected by the lead object. These two sets of data are verified, examined and compared to yield our final findings.

2.1 Process

1. The information in the data file is verified to determine whether the coincidence events show a linear relationship with the timestamp.
2. We compare each set of coincidence events in the same pair of CW, both with and without an object, to ensure consistency.
3. Temperature and pressure graphs are plotted to explain the “non-linear” relationship between a coincidence event and a timestamp.
4. Certain errors are detected and explained.
5. For all data sets, coincidence event rates are collected and processed to draw further conclusions.

2.2 Result & Analysis

E.g. D3B without object, D3T without object

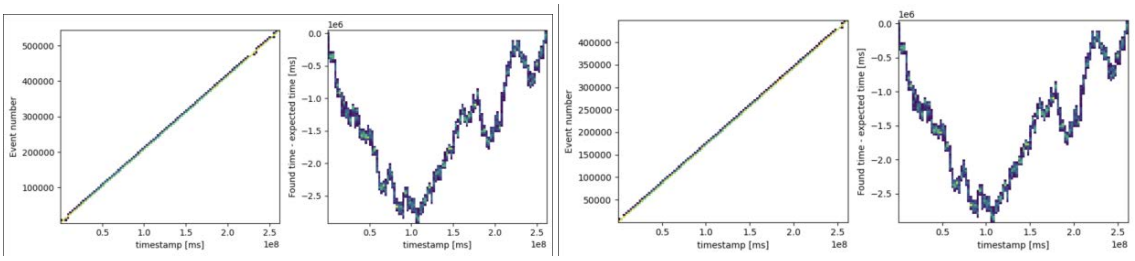

Figure 2 The correlation graph

The two graphs are randomly chosen to illustrate the general condition, and the coincidence rates do linearly correlate with the timestamp. The righthand-side graph demonstrates the shape of the relationship, and it is not exactly linear due to pressure and temperature differences. The same pair of CW shows the same result as we previously thought, but different pairs of CW shows different coincidence event number and shape of relation.

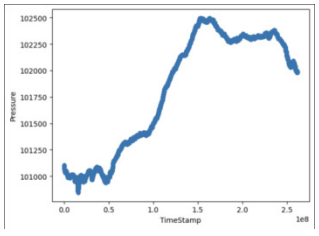

Figure 3 pressure and timestamp correlation

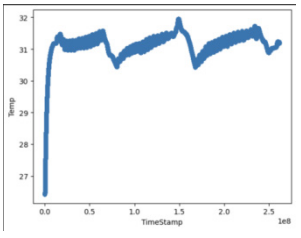

Figure 4 timestamp and temp correlation

These two graphs, the temperature and pressure graphs of D3B, contribute to the curved shape of the none-linear relationship between the coincidence and the timestamp. The rapid change in temperature in the graph could be attributed to the difference in day-night temperature, as the detection occurred over a period of days.

E.g. D2T with object

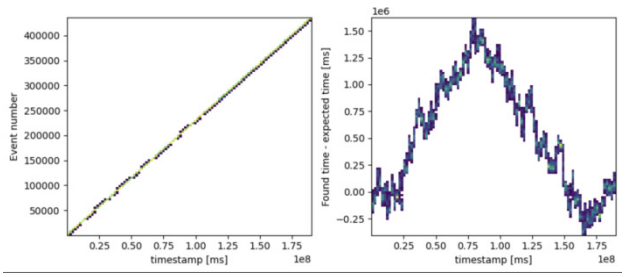

Figure 5 inaccuracies of the data

This graph illustrates certain inaccuracies in the data observed within the data file. The data file displays non-continuous coincidence events, with cracks appearing along a straight line. The cracks in the middle are the result of the CW's long-term functioning, so some slight variations occurred in the machine.

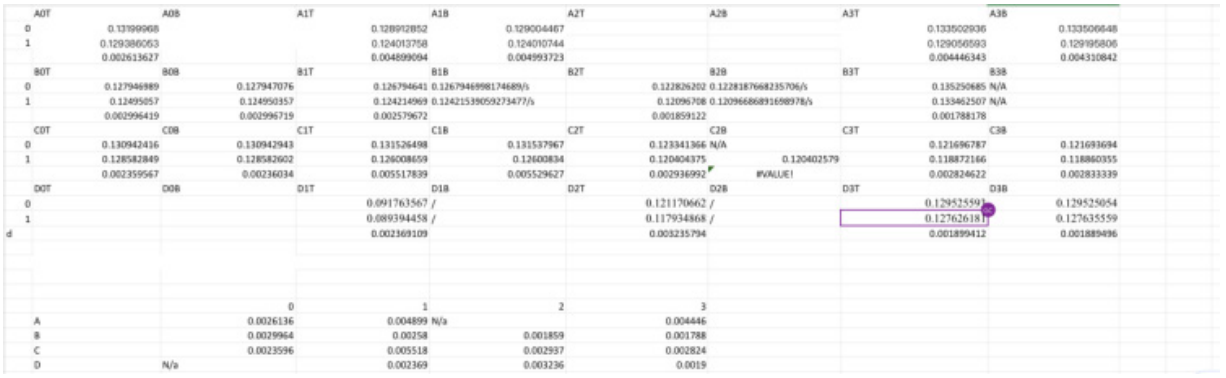

Figure 6 coincidence event rates

This plotted Excel graph contains all the coincidence event rates listed, and their differences are plotted in the lower section. The detectors for A2T, A2B, A3T, D0T, D0B, D1T, D1B, and D2B do not have any information installed due to apparent storage errors on the memory card. The results of coincidence event rates are further analyzed with graphs that reveal more useful information since this plain diagram is not too informative.

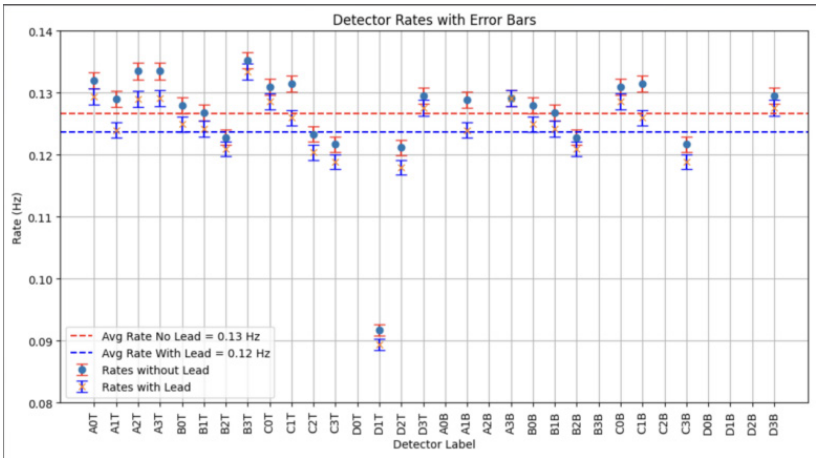

Figure 7 comparison between the coincidence rates

This graph provides a more accurate representation of the coincidence rates. It is clear that object detectors experience lower rates than those without object detectors, and this is due to fewer muons. Some coincidence rates exist outside of the drawn error bar, which can be attributed to the fact that different CW have varying thresholds for identifying muons as signals. This set of data is not regulated, so more calculation is needed to present a more accurate conclusion.

2.3 Section Conclusion

The above analysis demonstrates some initial development we had about the 16 pairs of CW, and we can see a clear distinction between the with-object CWs and the without-object CWs. We also identified certain specialties about the data file and examined some errors.

3. CW timestamp modification

Due to the differing startup times and recording frequencies of each cosmic watch, the timestamps correspond-

ISSN 2959-6157

ing to coincidences in the data received by each cosmic watch do not reflect events occurring at the same moment. Therefore, the first step in this experiment is to identify the true coincidences corresponding to the timestamps for each cosmic watch. To correct the time differences between each continuous wave, we perform data analysis on two configurations: one where the cosmic watches are placed vertically above and below each other, and another where they are placed at an inclined vertical position.

3.1 Setup

The setup is shown in Figure 8 and Figure 9:

Figure 8: The data will come for two 1*2 arrays of detectors. I will probably take data for 10 days with an object and 10 days without an object.

Figure 9: Have a 4x4 array of cosmic watches, and we recorded data from these cosmic watches both with and without an absorber.

3.2 Process and Result:

1) To validate the data obtained from the CW as cracks may occur in the middle due to problems in the CW. For the CW one useful plot to make is a scatter plot of time stamp vs event number. By drawing the frequency plot, we conclude that 90% of the data is noise. Then we narrow the number line to compare the shape of the coincidence distribution, and find that the true coincidence has a peak (We get a linear relationship between them(Figure 10))

2) T45 and T02 are taken as examples to analyze the relationship between the time difference and the frequency. Plot 1 percent, 2 percent, 3.3 percent, and 10 percent of the data from the two files as bar graphs.(Figure 11)

3) According to the above four figures(1/100, 1/50, 1/30, 1/10), the real time difference is roughly in the interval of (-500, 0), and then the image of time difference and frequency is drawn at (-500, 0). The conclusion we want to get is this—the real time difference between T02 and T45 is about –200. But analysis is error (Can't tell from this plot. Needs more data.). Moreover, there was some bias in the data selection, and the two cw placed above and below should be analyzed first.(Figure 12)

4) The relationship between time difference and frequency was analyzed again for T45 and B45(Figure 13). According to the above four figures(1/100, 1/50, 1/30, 1/10), the real time difference is roughly in the interval of (500,1500), and then the image of time difference and frequency is drawn at (500, 1500)(Figure 14).

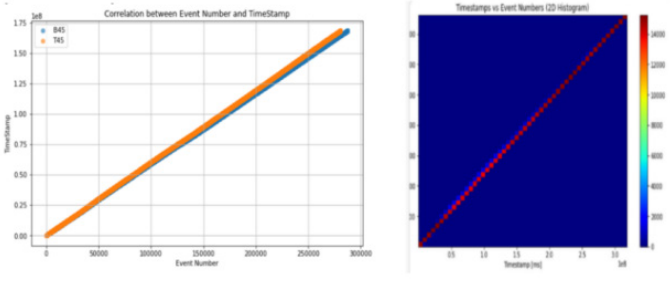

Figure 10: Timestamp vs Event number

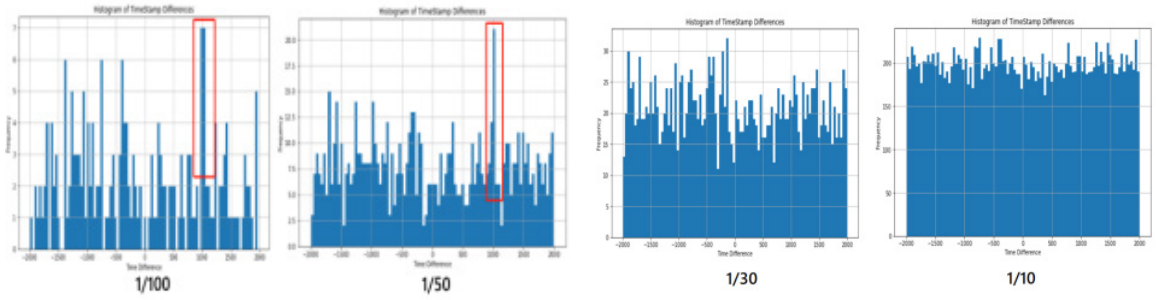

Figure 11: Histogram with timestamp difference; the fraction represents the percentage of overall data chose to analyze

3.3 Section Conclusion:

We successfully identified the startup time difference for the vertically placed cosmic watches. We will discuss how to use this data to correct the time differences among the cosmic watches. Next, we need to consider the impact of air pressure on the coincidences.

4. Pressure Correction

Since muons are unstable particles that might experience decay or reaction with atmospheric particles, the rate of coincidence/ muon detection is correlated to the level of atmospheric pressure the CW functions. While different CWs detected different pressure level. Especially for machines that functions during different time periods, the pressure difference detected are up to 500Pa. Therefore to eliminate this confounding variable and to focus on absorber's influence on coincidence rate, we need to come up with a plan to balance out the effect of pressure on coincidence rate.

4.1 Process:

1. We divide the data in each CW files into 1-hour segments and calculated:
l CR_hour & P_hour - 1-hour's average coincidence rate and pressure for each file
l CR_All & P_All - Overall average coincidence rate and pressure of all CW data (there's with observer & without observer version)
2. Graph ratio of CR_hour to CR_all on the y-axis and ratio of P_hour to P_all on the x axis.
The ratio graph gives an insight of the relationship between coincidence rate and pressure
3. Next, we need some algebra to find the equation for pressure correction

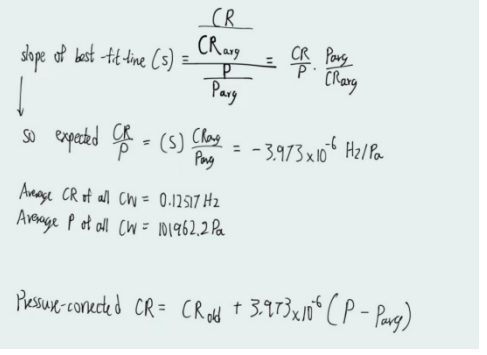

Figure 12. obtain equation for pressure correction

The slope from the ratio graph would be the expected ratio of coincidence rate over pressure times P_All / CR_All. With the expected ratio of CR/P known, we can then obtain the equation for pressure-corrected CR which equals the observed CR + the expected ratio times the difference between the observed pressure and average pressure.
4. Graph the pressure_corrected CR vs. Pressure for each hour-segmented data to check the product of pressure correction
5. Use the same pressure correction equation to modify the coincidence rate for all CW file. (Use the average pressure of each pair of CW for "P" in the equation)
6. Graph the heatmap with the pressure corrected Coincidence Rate

ISSN 2959-6157

4.2 Result & Analysis

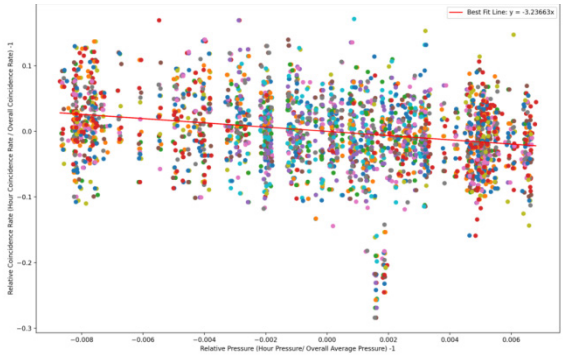

Figure 13: Relative Coincidence Rate vs. Relative Pressure

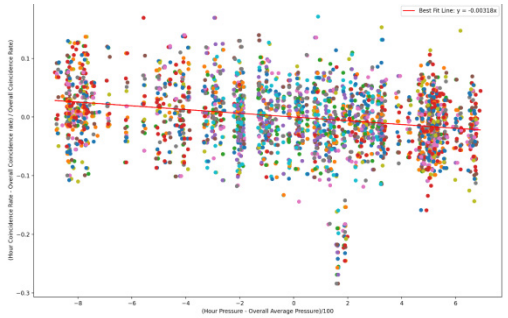

Figure 14: Percentage difference of coincidence rate vs. Difference of pressure

It's the ratio graph(Figure 13) plotted with CW detected data. The graph shows a relationship as we expected. The negative correlation suggests coincidence rate decreases as atmospheric pressure increases.

The graph(Figure 14) above is modified to make comparison with other research's finding. Here's another graph with same variable plotted (also intended to show correlation between coincidence rate and pressure). The y axis is percentage difference of detected CR to the average CR, while the x-axis is the difference between observed pressure to average pressure.

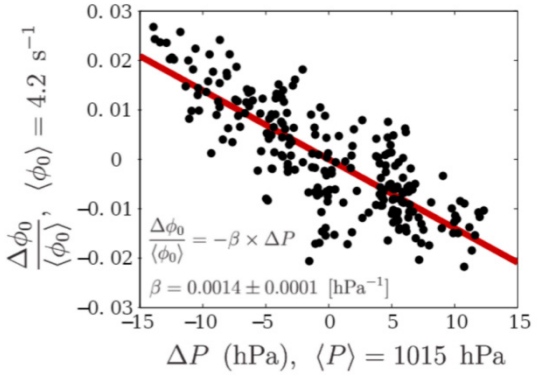

Figure 15 Percentage difference of coincidence rate vs. Difference of pressure

* The graph is from the study by "Jourde, Kevin & Gibert, Dominique & Marteau, J. & de Bremond d'Ars, Jean & Gardien, Serge & Girerd, Claude & Ianigro, Jean-Christophe. (2015). Monitoring temporal opacity fluctuations of large structures with muon tomography : a calibration experiment using a water tower tank. Scientific Reports. 6. 10.1038/srep23054. "

As can see, the slope of two graphs have some obvious differences, our data's slope is two times the slope from other research. But the difference is reasonable since the referred study used larger detector that produce different data, so some level of discrepancy is acceptable. Besides, the slope has the same scale of magnitude, which again, shows the data is reasonable.

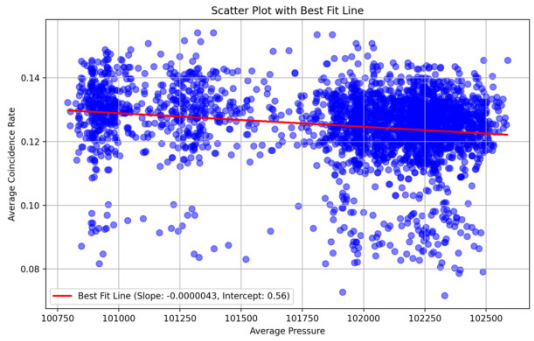

Figure 16: Coincidence Rate vs. Pressure

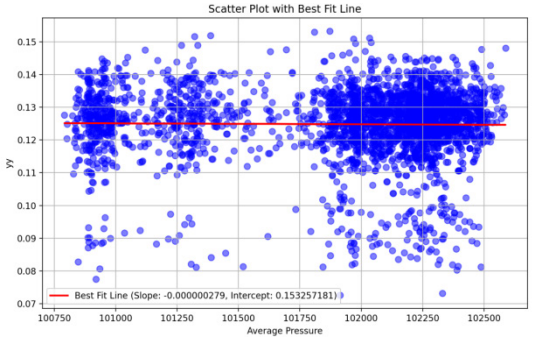

Figure 17: Corrected Coincidence Rate vs. Pressure

The graphs compares the detected CR and pressure corrected CR, also shows their relationship with pressure. The corrected version shows a nearly horizontal slope, indicates pressure's influence have been balanced. However, the pressure-corrected graph still has a slightly negative slope, it can also be explained since the With absorber data tends to has higher pressure and certainly has lower coincidence rate due to the absorber's effect, so a negative slope should have appeared even with pressure corrected.

Finally, we applied the pressure correction equation to adjust the data and plot the pressure-corrected heatmap with the uncertainty labeled.

The plot is graphed in With absorber CR/ Without absorber CR ratio

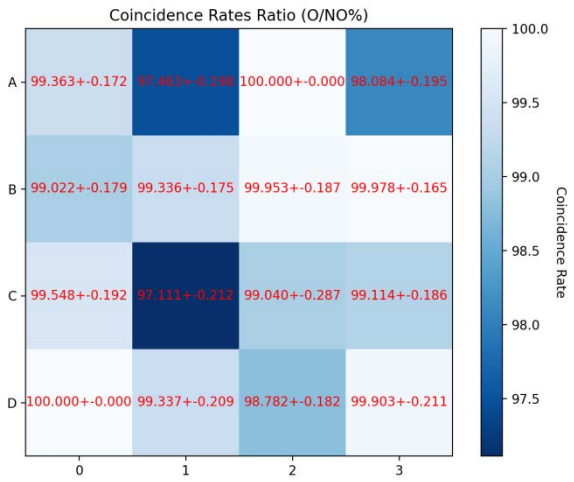

Figure 18: Coincidence Rate Radio (O/NO%) (with correction)

Below is the version for comparison

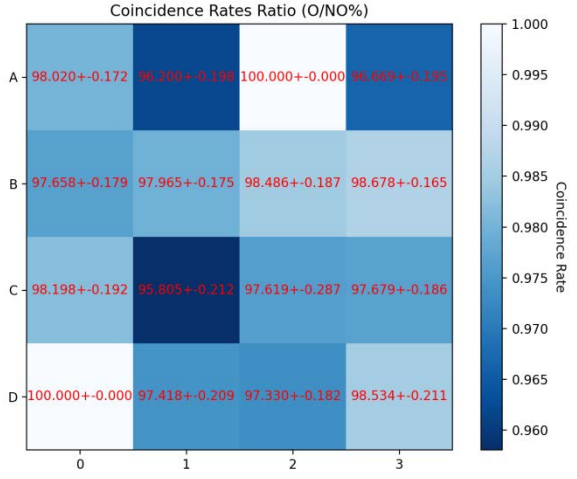

Figure 19: Coincidence Rates Ratio (O/NO%) (without correction)

As can be seen, the corrected version shows smaller gap between With & without absorber coincidence rate. The result is expected since the significant pressure difference mostly occurs between with absorber and without absorber data, so correcting effect of pressure should produce less discrepancy between two versions.

4.3 Section Conclusion

In this section, we provide the procedure of pressure correction and explain the mechanic. We also analyzed the result and displayed graph, while explained why the plot makes sense and the potential error behind.

5. Monte Carlo Simulation

Previous part are all results from actual experiment, this part will introduce a simulation that simulate what will happen when muons hit absorber and whether it will be detected by cosmic watches. This simulation uses Monte Carlo Simulation, (KENTON, 2024), a model used for potential random variables to estimate variety results. We run this simulation on 2 kinds of absorber:

1) an absorber of size 10cm*25cm*5cm, which only covers partial of the plane.

2) an absorber of size 40cm*40Cm*5cm, which covers whole plane.

The purpose of this simulation is trying to see whether we can tell different shape and size of absorbers from the data and result of cosmic watches. (Heck, 1998)

5.1 Setup

The setup is shown in Figure 20.

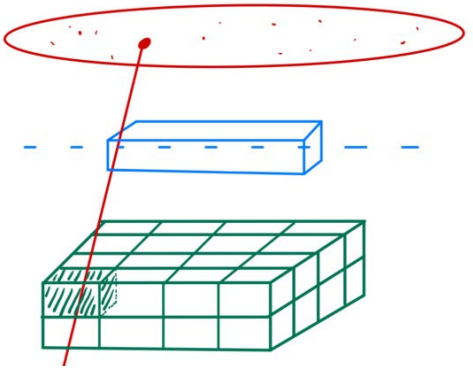

Figure 20: setup diagram for muon simulation

The red circle is the range where the muons come from, the blue box is the simulation of absorber, the green part represent 2 layers of cosmic watches, total in 16 pairs. Each cosmic watch is in size 6cm * 6cm * 6cm.

5.2 Process:

1) Generate muons. For each muon, randomly generate the position for it inside the range of the circle (the circle has diameter 50cm, and centered at (0,0,10)), then randomly generate a direction for each muon, this direction follows a cos^2 distribution.

2) Check whether muons hit absorber, check whether muons hit absorber. If muon hit absorber and being absorbed, this muon terminates and no longer continue; if not hit absorber, nothing happens and continue its path; if hit absorber and not being absorbed, continue its path, whether the muon will be absorber or not when passing through the absorber were depends on the length it go through inside the absorber, i.e. the attenuation length. Total number

ISSN 2959-6157

of muons passing through the absorber decreases exponentially with the pathlength. Also notice that the energy carried by muons should also change depends on actual case, but for simplicity of code and direct result, we did not consider the change in energy in the simulation.

3) Check if the muons are detected by cosmic pairs. If yes, record this hit.

5.3 Result

Run this simulation with 30000000 muons and we get following results. The graph shows the heatmap of how many muons are detected by each cosmic watch pair. The left graph shows the simulation with absorber and the right side shows the simulation without the absorber.

Figure 21 shows the result from partial absorber of size 10cm *25cm *5cm. The middle part is shallower than around, less muons are detected. This shape shown on heatmap is roughly the same as the absorber's shape. And for the graph without absorber at all, the numbers of detected muons are evenly distributed.

Figure 26 shows the result form absorber of size 40cm *40cm *5cm. The whole graph is shallower than without absorber one, less muons are detected. This shape shown on heatmap is roughly the same as the absorber's shape.

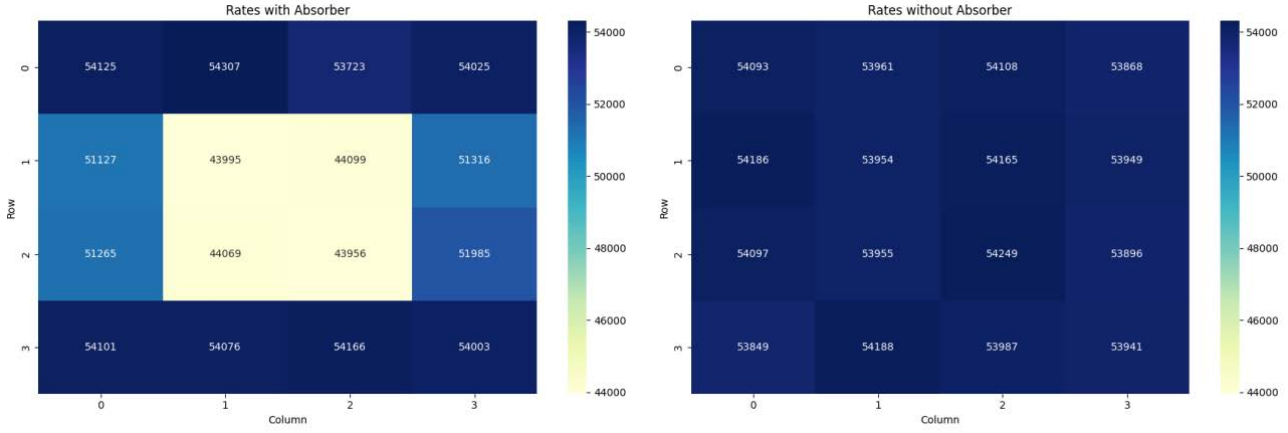

Figure 21 Heatmap for coincidence number (with absorber size 10*25*5cm)

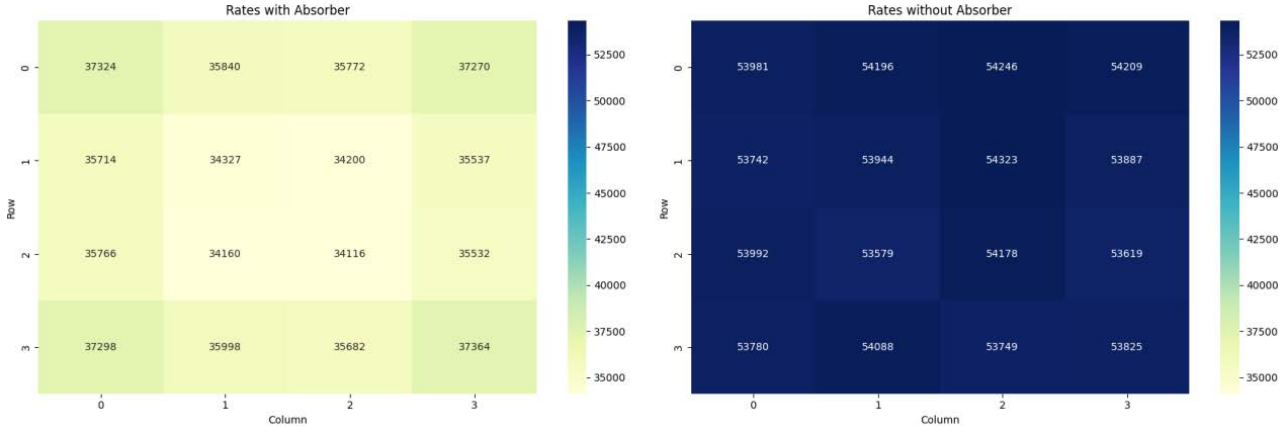

Figure 22 Heatmap for coincidence number (with absorber size 40*40*5cm)

5.4 Discussion:

This simulation successfully shows the pattern for different size of absorber, represented by less muons are detected at the position where absorber is placed, might provide useful insight to analysis of actual data.

Acknowledgement

Chongen Huang, YaranYang, Zile Liu, Zaiye Wang, xiju Li contributed equally to this work and should be considered co-first authors .

References

Heck, D., Knapp, J., Capdevielle, J.N., Schatz, G., Thouw, T., 1998. CORSIKA: A Monte Carlo Code to Simulate Extensive Air Showers. Forschungszentrum Karlsruhe GmbH, Karlsruhe.

High Resolution Muon Tomography using a Portable Prototype Muon Telescope S. Ahmed Shanto, R. Perez, M. Moosajee, S. Cano, C. Moreno Advanced Particle Detector Laboratory, Department of Physics and Astronomy, Texas Tech University

Jourde, Kevin & Gibert, Dominique & Marteau, J. & de Bremond d'Ars, Jean & Gardien, Serge & Girerd, Claude & Ianigro, Jean-Christophe. (2015). Monitoring temporal opacity fluctuations of large structures with muon tomography : a calibration experiment using a water tower tank. Scientific Reports. 6. 10.1038/srep23054.

Liu, Mira, and Patrick La Riviere. "Simulation of Muon Tomography Projections to Image the Pyramids of Giza." ArXiv, February 27, 2024, arXiv:2402.17909v1.